Enhanced absorption properties of ordered mesoporous carbon/Co-doped ordered mesoporous carbon double-layer absorbers*

Guo Shao-Li(郭绍丽), Wang Liu-Ding(王六定)†, Wang Yi-Ming (王一明), Wu Hong-Jing(吴宏景), and Shen Zhong-Yuan(沈中元)

School of Science, Northwestern Polytechnical University, Xi'an 710072, *China*

(Received 9 July 2012; revised manuscript received 28 November 2012)

Ordered mesoporous carbon (OMC) and metal-doped (M-doped) OMC composites are prepared, and their electromagnetic (EM) parameters are measured. Using the measured EM parameters we calculate the EM wave absorption properties of a double-layer absorber, which is composed of OMC as an absorbing layer and M-doped OMC as the matching layer. The calculated results show that the EM wave absorption performance of OMC/OMC–Co (2.2 mm/2.1 mm) is improved remarkably. The obtained effective absorption bandwidth is up to 10.3 GHz and the minimum reflection loss reaches −47.6 dB at 14.3 GHz. The enhanced absorption property of OMC/OMC–Co can be attributed to the impedance match between the air and the absorber. Moreover, it can be found that for the absorber with a given matching layer, a larger value of $\Delta\tan\delta_\varepsilon (= \tan\delta_{\varepsilon\ \text{absorbing}} - \tan\delta_{\varepsilon\ \text{matching}})$ can induce better absorption performance, indicating that the difference in impedance between the absorbing layer and the matching layer plays an important role in improving the absorption property of double-layer absorbers.

Keywords: ordered mesoporous carbon, electromagnetic wave absorption, double-layer absorber

PACS: 41.20.Gz, 75.70.Cn, 77.22.Gm **DOI:** 10.1088/1674-1056/22/4/044101

1. Introduction

Until now, electromagnetic interference (EMI) problems in the frequency range 2 GHz–18 GHz have received considerable attention. The design and fabrication of electromagnetic (EM) wave absorbers which are lightweight and thin, as well as having a wide effective absorption bandwidth (Δf_{eff}), i.e. reflection loss (RL) < -10 dB, have been widely investigated.[1–5] Theoretically, a double-layer absorber would exhibit better microwave absorption performance than a single-layer one. Firstly, the matching layer allows most of the incident EM waves to easily enter into the absorber. Secondly, the interface between the matching layer and the absorbing layer can enhance the chance of multi-reflection and scattering, which is in favor of EM wave attenuation. Feng *et al*.[6] reported on a double-layer absorber composed of carbonyl iron and barium ferrite with RL < -13 dB in a range of 6 GHz–18 GHz and RL < -8 dB in a range of 2 GHz–18 GHz. Hou *et al*.[1] found that the maximum Δf_{eff} of a double-layer absorber composed of CNT and Ni-doped CNT is 5.28 GHz. Moreover, it has been reported that the optimized Δf_{eff} of a carbon black (CB)/MnO_2 double-layer absorber is 8.7 GHz.[2]

Owing to a high specific surface area, tunable pore size and periodic pore arrangement, OMC has potential applications in many fields, such as separation,[7] catalysis,[8] electrode materials,[9] energy storage,[10] etc. Previous reports[11–13] demonstrated that OMC is a promising candidate for fabricating high-efficiency and lightweight absorbers. On the one hand, the porous periodic structure is in favor of the reduction of the density as well as the attenuation of the incident EM waves. On the other, by dispersing ferromagnetic metal components into the pores of OMC, the magnetic and dielectric losses of metal-doped (M-doped) composites could be well matched, leading to microwave absorption enhancement.

In this paper, absorbents of OMC and M-doped (Co, Fe, Ni, and Al) OMC are fabricated. The EM parameters are measured, each as a function of frequency. Based on transmission-line theory and the measured EM parameters, the absorption properties of the double-layer absorbers are calculated.

2. Experiment

2.1. Materials and preparation

OMC was synthesized using mesoporous silica (SBA-15) as the hard template. SBA-15 was prepared according to the following synthesis procedure reported by Zhao *et al*.[14] Then, the calcined SBA-15 (1 g) was impregnated with a solution obtained by dissolving 1.25 g of sucrose and 0.14 g of H_2SO_4 in 5 g of water.[15] The mixture was dried at 80 °C and 160 °C for 6 h, respectively. After the treatment, the sample turned

*Project supported by the National Natural Science Foundation of China (Grant Nos. 50771082 and 60776822), the Doctorate Foundation (Grant No. CX201207), the Graduate Starting Seed Fund of Northwestern Polytechnical University (Grant No. Z2011011), the Natural Science Foundation of Shaanxi Province, China (Grant No. 2012JM1009), and the Scientific Research Program Funded by Shaanxi Provincial Educational Department, China (Grant No. 12JK0984).

†Corresponding author. E-mail: wangld@nwpu.edu.cn

© 2013 Chinese Physical Society and IOP Publishing Ltd

dark brown. The pretreated sample was again treated at 80 °C and 160 °C successively after the addition of 0.8 g of sucrose, 0.09 g of $H_2SO_4$and 5 g of water. The carbonization was completed by pyrolysis at 900 °C under N_2 atmosphere. Then, the silica template was removed after 120 min ultrasonic irradiation in sodium hydroxide aqueous solution (2 M). Finally, the OMC was filtered, washed thoroughly with distilled water, and dried at 80 °C for 12 h.

M-doped OMC was prepared as mentioned in our previous report.[12] Typically, 0.5 g of OMC was added into 20 mol of aqueous solution of nitrate (Co/Fe/Ni/Al) (0.1 M), and then the mixture was ultrasonically irradiated at room temperature for 2 h. Subsequently, the metal-contained OMC was filtered, washed thoroughly with distilled water and ethanol, and dried at 80 °C for 12 h. The above-mentioned procedures were repeated several times until the weight of the dried solid did not change. The resulting material was calcined at 300 °C for 4 h.

2.2. Characterization

The samples were characterized by X-ray photoelectron spectroscopy (XPS) (VP-II 5000, ULVAC-PHI, Japan), X-ray diffraction (XRD) (D/MAX, Rigaku, Japan), scanning electron microscopy (SEM) (JSM-5610LV, JEOL, Japan), and transmission electron microscopy (TEM) (JEM-2100, JEOL, Japan).

For the measurement of the EM parameters using a vector network analyzer (HP 8720B), the powders were mixed with paraffin wax (weight ratio 1:9) and pressed into a toroid with an outer diameter of 7.0 mm, inner diameter of 3.04 mm, and a thickness of 3.0 mm. The as-prepared composites are defined as OMC, OMC–Fe, OMC–Co, OMC–Ni, and OMC–Al, respectively.

3. Results and discussion

3.1. Morphology

The TEM and SEM micrographs of the samples are shown in Fig. 1. It can be clearly seen from Figs. 1(a) and 1(b) that parallel pore channels are highly arranged in the [110] direction, indicating an excellent ordered structure of mesoporous carbon. Corresponding to the TEM results, the low-angle XRD pattern of OMC–Co (Fig. 1(d)) shows a diffraction peak around 2θ of 1.0°, which belongs to a typical 2D hexagonal space group ($p6mm$).[13,15] In addition, small dark grains belonging to the cobalt species in Fig. 1(b) are well dispersed in OMC, which is in accordance with the energy-dispersive spectrometry (EDS) spectrum (inset of Fig. 2(a)). Figure 2(b) shows the Co 2p XPS spectrum of the OMC–Co composite, in which the two peaks at 796.5 eV and 781.2 eV represent the Co $2p_{1/2}$ and Co $2p_{3/2}$ spin–orbit of CoO, respectively. The other two peaks at 804.8 eV and 787.6 eV are assigned to cobalt species Co_2O_3. Therefore, it can be inferred that the Co species that are doped into OMC are mainly CoO and Co_2O_3.

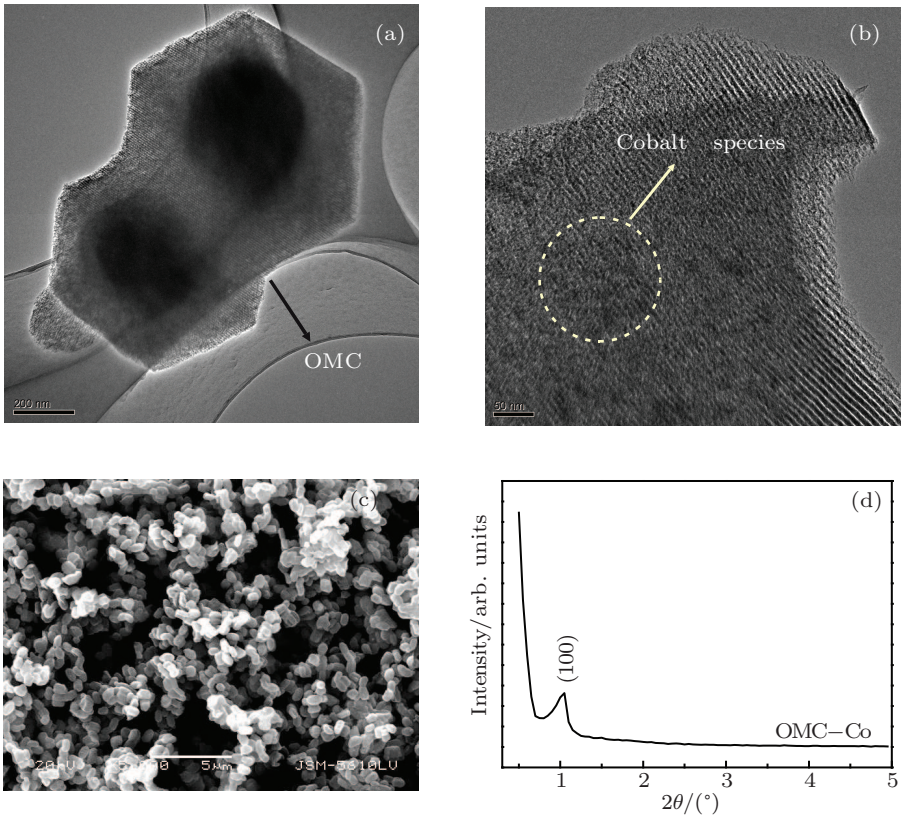


Fig. 1. TEM images of (a) OMC and (b) OMC–Co. (c) SEM image and (d) low-angle XRD pattern of OMC–Co.

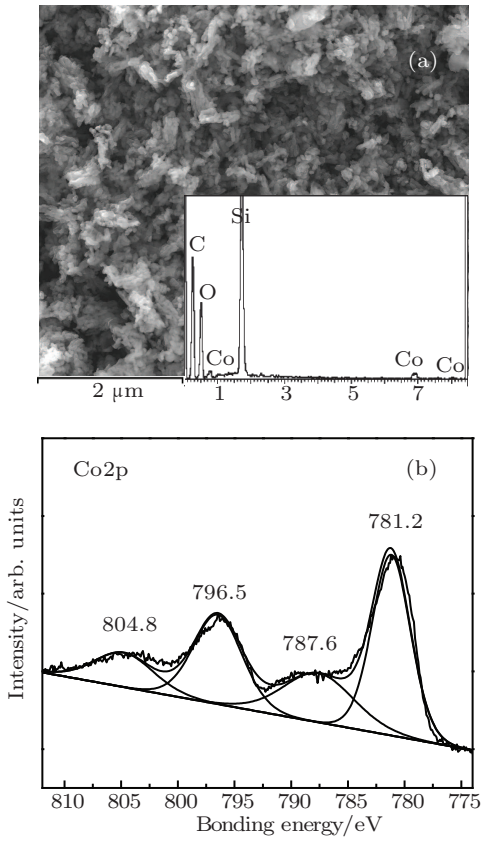


Fig. 2. (a) SEM image of OMC–Co (the inset shows the EDS of the area), and (b) XPS spectrum of the Co 2p region for OMC–Co.

3.2. Electromagnetic properties of OMC and M-doped OMC

Figures 3 and 4 show the complex relative permittivity ($\varepsilon_r = \varepsilon' - j\varepsilon''$) and permeability ($\mu_r = \mu' - j\mu''$) measured for the as-prepared composites. Figure 3 reveals that OMC is a typical dielectric loss material due to high dielectric loss and the weak magnetic characteristics as demonstrated by previous reports.[11,13] It can be seen from Fig. 4(a) that for OMC–Al and OMC–Ni, the values of ε' decrease gradually as the frequency increases, and each curve shows one main peak at about 15 GHz. However, the values of ε' for OMC–Fe and OMC–Co are almost independent of frequency except for small fluctuations in the vicinity of 13 GHz. As shown in Fig. 4(b), the values of ε'' for OMC–Ni and OMC–Al decrease from about 12 to 5 and 7 to 3 between 2 GHz and 7 GHz, and fluctuate in the higher frequency range. In particular, there are resonance peaks in the ε''–f curve at around 15 GHz. In general, the dielectric loss of M-doped OMC/paraffin composites can be ascribed to the polarization relaxation which arises from the existence of the mesopores, the interfacial polarization relaxation at the interfaces among OMC, metal components and paraffin, as well as the leakage conductance. In the low-frequency range, the dielectric losses of OMC–Ni and OMC–Al are probably dominated by the leakage conductance loss and the interfacial polarization. For the higher-frequency regime, the interfacial polarization is inhibited by the relaxation lag,[2,6] and thus the values of ε'' decrease with increasing frequency. The above-mentioned high-frequency resonances of ε'' can be attributed to atomic and electronic polarizations.[16] In addition, the values of ε'' for OMC–Co and OMC–Fe approximate to 0, except for a major peak at about 13.5 GHz, indicating a typical dielectric resonance behavior for M-doped absorbents. As shown in Figs. 4(c) and 4(d), the values of μ' for the M-doped OMC samples approximate to 1, while the corresponding μ'' values are negative almost within the whole frequency range as reported by Zhou *et al.*,[13] and each curve exhibits an obvious resonance peak at about 15 GHz. Generally, a negative μ'' value can be considered as magnetic energy going out of the absorber.[11,13] In OMC material, the electron current can easily be induced in order to resist the applied magnetic field, and then converted into dissipative current.[13,17] The resonance peak may be related to natural resonance originating from the shape effect of the doped-metal components.[11]

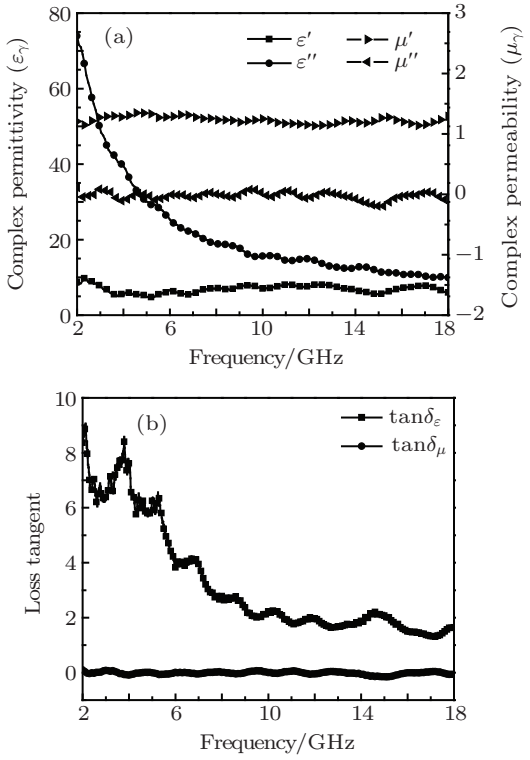


Fig. 3. (a) Values of complex permittivity (ε' and ε'') and permeability (μ' and μ''), and (b) the dielectric loss tangent ($\tan\delta_\varepsilon$) and magnetic loss tangent ($\tan\delta_\mu$) of OMC versus frequency.

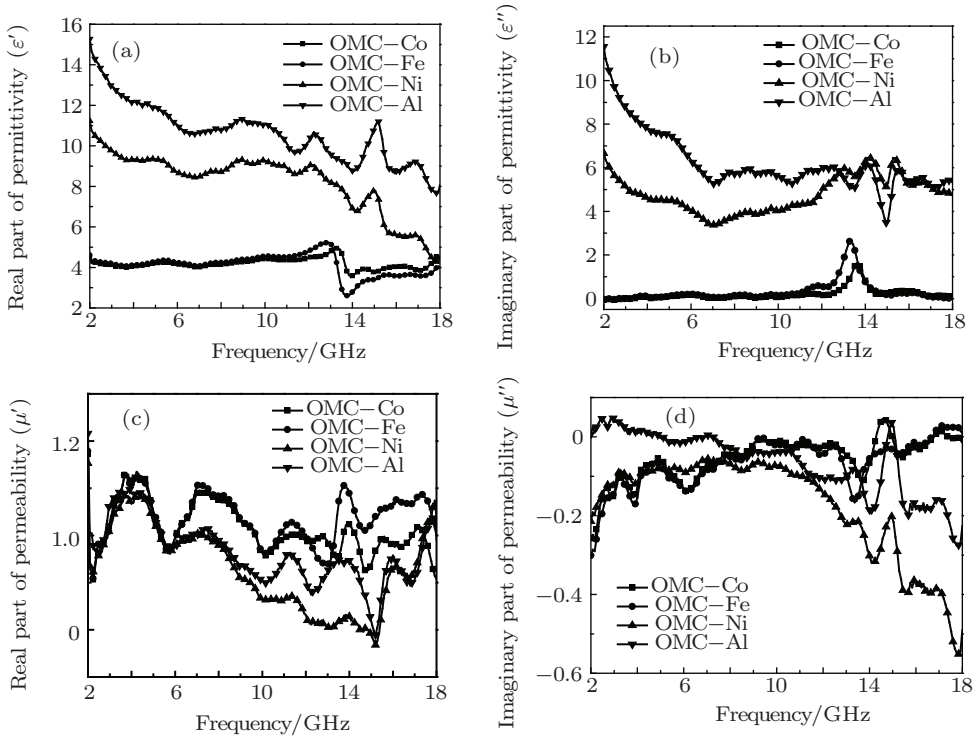


Fig. 4. EM parameters (a) ε', (b) ε'', (c) μ', and (d) μ'' of M-doped composites versus frequency.

The loss tangents of the samples containing metal components are shown in Fig. 5. It can be clearly seen that the dielectric loss is the main microwave absorbing mechanism of the M-doped OMC.

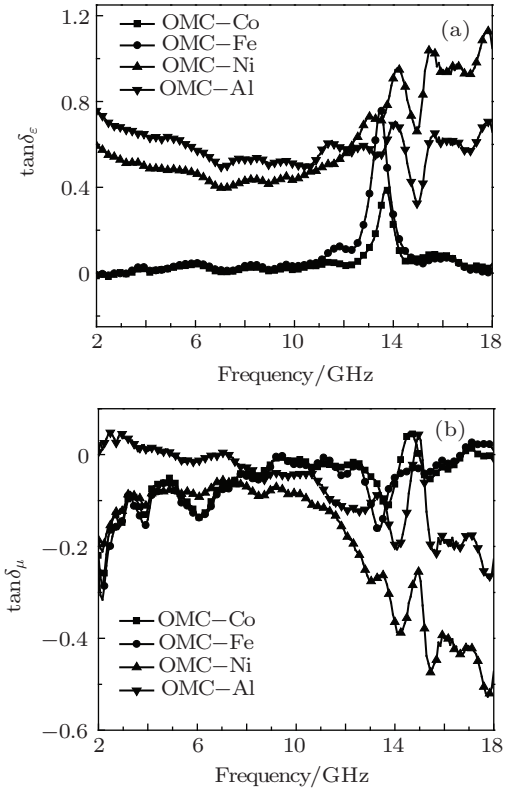


Fig. 5. Loss tangents of the M-doped OMC: (a) $\tan\delta_\varepsilon$ and (b) $\tan\delta_\mu$.

3.3. Microwave absorption properties of the double-layer absorbers

A sketch of a proposed double-layer absorber is shown in Fig. 6, where layer A represents the absorbing layer and layer B denotes the matching layer. Based on transmission-line theory, the EM wave absorption property of a double-layer absorber is characterized by RL, which is calculated as follows:

$$\mathrm{RL}(\mathrm{dB}) = 20\log\left|\frac{Z-Z_0}{Z+Z_0}\right|, \tag{1}$$

$$Z = Z_2\frac{Z_1\eta_1 + Z_2\eta_2}{Z_2 + Z_1\eta_1\eta_2}, \tag{2}$$

$$Z_n = Z_0\sqrt{\frac{\mu_{rn}}{\varepsilon_{rn}}}, \quad (n=1,2), \tag{3}$$

$$\eta_n = \tanh(\mathrm{j}2\pi f d_n/c)\sqrt{\mu_{rn}\varepsilon_{rn}}, \quad (n=1,2), \tag{4}$$

where Z_0 is the impedance of the free space (377 Ω); Z_1 and Z_2 are the characteristic impedances of the absorbing layer and the matching layer, respectively; c is the velocity of light, f the frequency of the incident EM wave, and d_n $(n = 1, 2)$ the thickness of each layer.[6]

The RLs for M-doped single-layer absorbers are shown in Fig. 7(a). Compared with OMC–Al and OMC–Ni, OMC–Co and OMC–Fe exhibit weak absorption abilities. However, the absorption properties of the double-layer absorber composed of OMC as the absorbing layer and OMC–Co (Fe) as the matching layer (i.e., OMC/OMC–Co (Fe)) are remarkably enhanced (Fig. 7(b)). In particular, OMC/OMC–Co (2.2 mm/2.1 mm) has the minimum RL of −47.6 dB at 14.3 GHz and the Δf_{eff} is up to 10.3 GHz (Fig. 8).

The Δf_{eff} values of the OMC/OMC–Fe, OMC/OMC–Ni, and OMC/OMC–Al double-layer absorbers are 10.2 GHz, 7.6 GHz, and 7.2 GHz, respectively. The results correspond with the impedance matching theory and fully highlight the structural advantage of the double-layer absorber. Firstly, the lower ε' OMC–Co value is crucial for the counterbalancing of permeability and permittivity, and for reducing the reflection coefficient of the absorber.[16] Secondly, due to the weak absorption property of OMC–Co, most of the incident EM waves can contact the interface between the two layers and then be multi-reflected, with the result that the attenuation of the EM wave is evidently enhanced. In particular, the absorption property of OMC/OMC–Co is better than that of the earlier reported double-layer absorbers (Table 1).

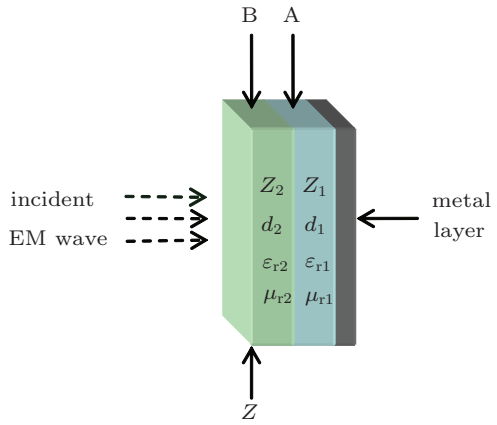


Fig. 6. (color online) Sketch of a double-layer absorber.

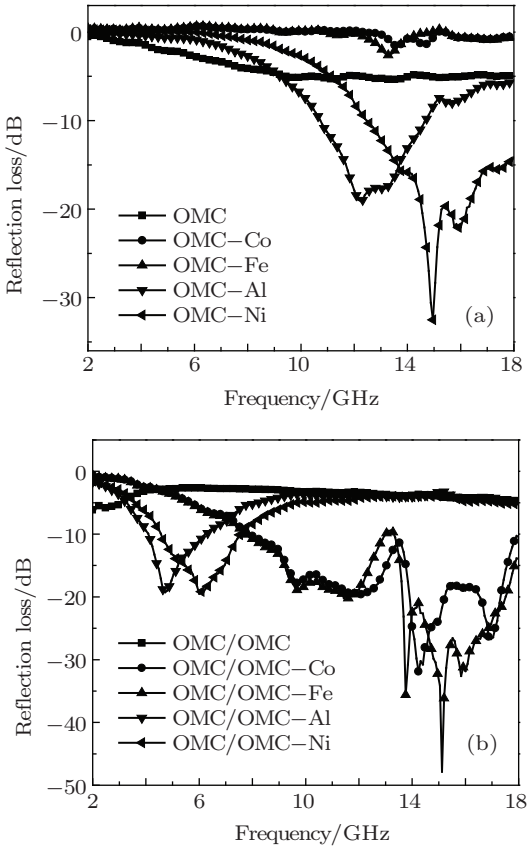


Fig. 7. (a) RLs of the M-doped single-layer absorbers (2 mm) and (b) the corresponding double-layer absorbers (2 mm, 2 mm).

Table 1. The EM wave absorption properties of various double-layer absorbers.

Matching layer	Absorbing layer	Bandwidth/GHz (RL< −10 dB)	Minimal RL/dB	Refs.
OMC/Co (2.1 mm)	OMC (2.2 mm)	10.3	–47.6	this work
MWCNTs (2 mm)	MWCNTs/RM (2 mm)	5.28	–21.04	[1]
MnO_2 (2 mm)	CB (2 mm)	8.7	–22	[2]
$BaTiO_3$ (0.2 mm)	$BaTiO_3$/CI (1.2 mm)	4.0	–59	[18]

Furthermore, we infer that for a double-layer absorber with a given matching layer, the impedance value of the absorbing layer is the key factor in EM wave absorption. To confirm this, we design a series of double-layer absorbers, each of which is composed of OMC–Co as the matching layer (2 mm) OMC and M-doped OMC as the absorbing layer (2 mm), respectively. As for the low magnetic loss absorbent, the complex permittivity is critical for the characteristic impedance (Z) of each layer (see Eq. (3)). As shown in Fig. 9, when the curves of RL versus $\Delta\tan\delta_\varepsilon (= \tan\delta_{\varepsilon\ \text{absorbing}} - \tan\delta_{\varepsilon\ \text{matching}})$ at frequencies of 13, 14, and 15 GHz are plotted, the former shows a decreasing trend with the increase of $\Delta\tan\delta_\varepsilon$, which implies that the absorption property of the double-layer absorber in our work is probably dominated by the impedance variation between the absorbing layer and the matching layer, i.e., the larger the difference, the better the absorption performance of the absorber.

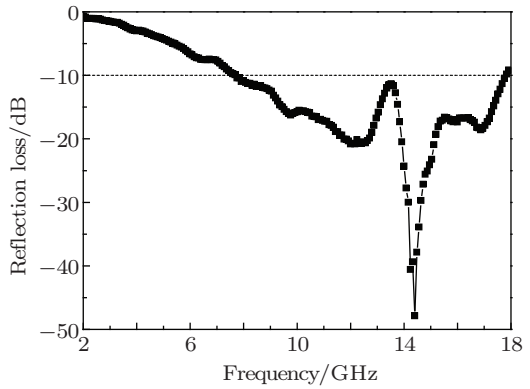


Fig. 8. RL versus frequency for an OMC/OMC–Co (2.2 mm/2.1 mm) double-layer absorber.

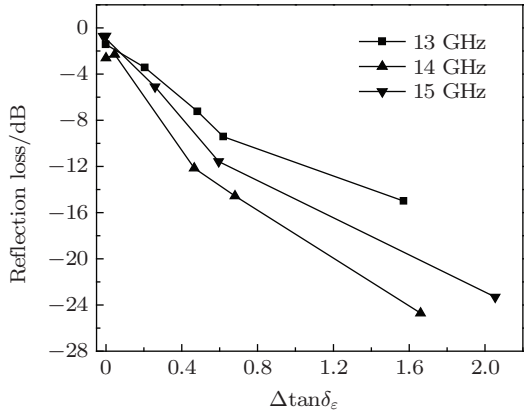


Fig. 9. RL versus $\Delta\tan\delta_\varepsilon$ for OMC–Co/(M-doped) OMC double-layer absorbers (2 mm, 2 mm) at a given frequency.

4. Conclusions

In this paper, we synthesized several OMC and M-doped OMC composites and measured their microwave absorption properties. On this basis, some OMC-based double-layer absorbers were designed and their EM wave absorbing properties were calculated. The results demonstrate that the absorbing properties of the double-layer absorbers in a frequency range of 2 GHz–18 GHz are markedly improved. The obtained effective absorption bandwidth of OMC/OMC–Co is 10.3 GHz and the minimum reflection loss reaches −47.6 dB at 14.3 GHz. The RL data indicate that OMC-based composite is a promising candidate for fabricating high-performance double-layer absorbers.

References

[1] Hou C L, Li T H, Zhao T K, Zhang W J and Cheng Y L 2012 *Mater. Design.* **33** 413
[2] Duan Y P, Yang Y, He M, Liu S H, Cui X D and Chen H F 2008 *J. Phys D: Appl. Phys.* **41** 125403
[3] Yan J F, You T G, Zhang Z Y, Tian J X, Yun J N and Zhao W 2011 *Chin. Phys. B* **20** 048102
[4] Liu T, Zhou P H, Liang D F and Deng L J 2012 *Chin. Phys. B* **21** 050302
[5] Jin H B, Li D, Cao M S, Dou Y K, Chen T, Wen B and Simeon A 2011 *Chin. Phys. Lett.* **28** 037701
[6] Feng Y B, Qiu T and Shen C Y 2007 *J. Magn. Magn. Mater.* **318** 8
[7] Zhai Y, Dou Y, Liu X, Tu B and Zhao D Y 2009 *J. Mater. Chem.* **19** 3292
[8] Cejka J 2003 *Appl. Catal. A* **254** 327
[9] Jiang X Y, Zhu L D, Yang D X, Mao X Y and Wu Y H 2009 *Electroanalysis* **21** 1617
[10] Peng X, Cao D P and Wang W C 2008 *J. Phys. Chem. C* **112** 13024
[11] Zhou J H, He J P, Li G X, Wang T, Sun D, Ding X C, Zhao J Q and Wu S H 2010 *J. Phys. Chem. C* **114** 7611
[12] Wu H J, Wang L D, Wang Y M, Guo S L and Shen Z Y 2012 *J. Alloys Compd.* **525** 82
[13] Zhou J H, He J P, Wang T, Li G X, Guo Y X, Zhao J Q and Ma Y 2011 *J. Alloys Compd.* **509** 8211
[14] Zhao D Y, Feng J L, Huo Q S, Melosh N, Fredrickson G H, Chmelka B F and Stucky G D 1998 *Science* **279** 548
[15] Jun S, Joo S H, Ryoo R, Kruk M, Jaroniec M, Liu Z, Ohsuna T and Terasaki O 2000 *J. Am. Chem. Soc.* **122** 10712
[16] Tang X, Tian Q, Zhao B Y and Hu K A 2007 *Mater. Sci. Eng. A* **445–446** 135
[17] Liu Q L, Zhang D and Fan T X 2008 *Appl. Phys. Lett.* **93** 013110
[18] Qing Y C, Zhou W C, Luo F and Zhu D M 2011 *J. Magn. Magn. Mater.* **323** 600